

## Water Absorption of Freeze-Dried Meat at Different Water Activities: a Multianalytical Approach Using Sorption Isotherm, Differential Scanning Calorimetry, and Nuclear Magnetic Resonance

LUCA VENTURI, PIETRO ROCCULI, CLAUDIO CAVANI, GIUSEPPE PLACUCCI,  
MARCO DALLA ROSA,\* AND MAURO A. CREMONINI\*

Department of Food Science, University of Bologna, Campus of Food Science, P.zza Goidanich 60,  
47023 Cesena, Italy

Hydration of freeze-dried chicken breast meat was followed in the water activity range of  $a_w = 0.12 - 0.99$  by a multianalytical approach comprising of sorption isotherm, differential scanning calorimetry (DSC), and nuclear magnetic resonance (NMR). The amount of frozen water and the shape of the  $T_2$ -relaxogram were evaluated at each water content by DSC and NMR, respectively. Data revealed an agreement between sorption isotherm and DSC experiments about the onset of bulk water ( $a_w = 0.83-0.86$ ), and NMR detected mobile water starting at  $a_w = 0.75$ . The origin of the short-transverse relaxation time part of the meat NMR signal was also reinvestigated through deuteration experiments and proposed to arise from protons belonging to plasticized matrix structures. It is proved both by  $D_2O$  experiments and by gravimetry that the extra protons not contributing to the water content in the NMR experiments are about 6.4% of the total proton NMR CPMG signal of meat.

**KEYWORDS:** NMR, DSC, sorption isotherm, freeze-dried meat,  $T_2$ -relaxograms

### INTRODUCTION

The mobility and availability of water in food systems depend on the extent of interactions between the aqueous phase and the biopolymers matrix (1). These parameters are of the utmost importance in food technology because the amount and physico-chemical behavior of water embedded in foods may trigger microbiological growth or even unwanted chemical reactions, thus lowering food quality and shelf life (2). It is thus highly desirable to attain a deep understanding of the interactions between water and food components to be able to produce clear-cut models and simple quality parameters that can be readily applied in the food industry.

A partial solution to the problem of assessing the degree of availability of water in food materials has been known since the 1950s, when Scott and Salwin independently introduced the now well-known concept of "water activity" ( $a_w$ ), whereby "boundness" to a food matrix is related to the relative vapor pressure of water (for a recent historical review see ref 3 and references therein); the studies on  $a_w$  led to the description of a "food stability map" (4) that is still widely used by the food industry as a stability indicator for food quality control and shelf life prediction. Although it is common to refer to the mobility and availability of water in foods or hygroscopic polymers with the expression "state of water" (see, for example, refs 5–8) it must be borne in

mind that, here, water is always as liquid as in the common liquid state, and it is held back by the capillary forces generated by the physical structure of the matrix beyond condensation.

As simple as it is (a single parameter describes the status of the whole embedded water),  $a_w$  suffers from a number of drawbacks that have been discussed in the literature along the years, many of them thoroughly reviewed in a famous paper by Slade and Levine (9). These researchers based their criticisms on the following points: (i) for  $a_w$  to be a meaningful descriptor of the water status, it is necessary that at thermal equilibrium the partial vapor pressure above the food system is the same as that of the embedded water (i.e., thermodynamic equilibrium is reached). This condition is generally fulfilled in diluted food systems but is hardly met in concentrated food systems, owing to the low diffusion rate of water with respect to the time scale of measurement. In these systems only a kinetic steady state is reached, which is at the basis of the known hysteresis effect in sorption and desorption isotherms; (ii) even if thermodynamic equilibrium were reached, no way would exist for extracting meaningful information from the sorption or desorption isotherms because the widely used BET (10) or GAB (11) equations are based on assumptions that do not hold good for food materials; (iii)  $a_w$  is not an absolute food stability predictor because spoilage at a certain measured  $a_w$  depends on food composition, physical structure, temperature, prior sample history, and even isotherm measurement methodology; (iv)  $a_w$  defined as relative vapor pressure can reflect only the surface properties of a system but not necessarily the molecular

\* To whom correspondence should be addressed. E-mail: mauro.cremonini@unibo.it, marco.dallarosa@unibo.it.

dynamics that take place in its interior. However, the authors agree that  $a_w$  and the parameters obtained from the isotherms may still retain some usefulness, provided they are used as mere empirical indicators for foods at well defined pressure and temperature conditions.

Given the theoretical weaknesses of the  $a_w$  and related isotherms approach, but also considering its widespread use in food engineering, it would be interesting to compare the data obtained from the sorption isotherm of a complex food matrix with those coming from other well-established techniques such as differential scanning calorimetry (DSC) and low-field nuclear magnetic resonance (LF-NMR). These techniques offer a different but complementary point of view for studying the dynamics of water in foods, as was recently demonstrated for several systems (12–16).

DSC is particularly well-suited for the characterization of water at a structural level. From the calorimetric point of view, water is studied in its “free” or “bound” state to the solid food matrix. Bound water is determined by DSC as the amount of unfrozen water left in a sample after it is cooled at low temperature below zero (17). As explained by Wolfe (18), the amount of unfrozen water depends in general on three effects: (i) the presence of small solutes, for example, ions; (ii) the presence of macromolecules and membranes, and (iii) the viscosity of the solution. The first two effects are thermodynamic in origin, whereas the latter is clearly related to the kinetics of the freezing process. Although the presence of small solutes depresses the freezing point because of the entropy of mixing, and it is roughly proportional to the number of solutes, the effect of mesoscopic objects (which are much less numerically) on the freezing point is related to the decreased energy of water in the vicinity of the hydrophilic groups (e.g., because of slower reorientation and hydrogen bonding). This effect extends “within a nanometer or so” from a hydrophilic surface so that “the quantity of unfrozen water may exceed the expected amount of “water of hydration” or “hydration shell” (18). DSC has been used to monitor the gross phase changes of water in polymeric networks (15) and in food systems such as honey (19) and meat (20).

Compared to DSC, foodstuff analysis via LF-NMR yields an additional degree of details for the description of the embedded water, albeit at the price of a more difficult interpretation of the results (for a recent review see ref 21). The measure of the transverse relaxation times ( $T_2$ ) often reveals a multicomponent behavior that reflects the existence of different proton pools within the sample (e.g., protons from the macromolecular matrix or fat or arising from water contained in different food compartments). A difficulty arises here about the assignment of each proton population to the corresponding chemical species, especially when no previous knowledge of the sample is available.

In this paper we set out to compare the description of the water status provided by  $a_w$ , DSC, and LF-NMR measurements during hydration of freeze-dried chicken breast meat taken here as a model system. Not only can meat be driven to span a large  $a_w$  range from complete dryness to complete hydration (the  $a_w$  of fresh meat is 0.99), but it is also well-characterized from both the NMR (22) and the DSC (23) point of view. To the best of our knowledge, this is the first time that this kind of multianalytical approach has been applied to the hydration of freeze-dried meat.

## MATERIALS AND METHODS

**Raw Material.** Twenty-four hours post mortem, boneless chicken breast meat was collected from a local commercial processing plant (Amadori Group, Cesena, Italy), packed on ice, and transported to the laboratory. Upon receipt at the laboratory, the two filets (pectoralis

major muscles) of each whole breast were separated, trimmed of excess fat and connective tissue, and held at 2–4 °C throughout handling and measurements. About 200 g were immediately analyzed for fresh sample measurements, and the remaining portion (about 4 kg) was freeze-dried.

**Freeze-drying.** Freeze-drying was performed using a freeze-dryer model Lio2000 (CinquePascal S.r.l., Milano, Italy). The initial sample temperature was –35 °C, well below the glass transition temperature of the tissue (around –16 °C (24)), and the pressure during the primary drying vacuum phase was 25.12 Pa. The freeze-drying process lasted for about 4 days, and the surface-to-volume ratio of the product was around 0.9 cm<sup>-1</sup>. Freeze-dried meat was packed under vacuum and stored at –18 °C until grounding and rehydration.

**Water Sorption Isotherm.** Freeze-dried meat (at about 0.5% residual water) was ground using an universal mill model M20 (IKA, Staufen, Germany) at a speed of 20 000 rpm for 15 s. During crushing, the milling chamber was maintained at 8–10 °C with a water-cooling system. The ground sample was immediately transferred into glass desiccators containing phosphorus pentoxide (P<sub>2</sub>O<sub>5</sub>) for two days to complete sample drying. A gravimetric method was employed for the determination of the sorption isotherm at 24 °C. Moisture equilibration took place inside 10 sterilized glass jars (hygrostats) containing 10 different saturated salt solutions covering relative humidity in the range 12–99% ( $a_w = 0.12, 0.33, 0.44, 0.57, 0.75, 0.86, 0.91, 0.94, 0.97,$  and 0.99). Dried samples of about 1 g were inserted into previously cleaned and oven-dried glass bottles, 10 mL in volume. Each hydration experiment comprised nine bottles. The bottles were kept half-open on a plastic net inside the hermetically closed hygrostats containing, on the bottom, different saturated salt solutions at the required  $a_w$  (25). The bottles were periodically taken (3 times a day) and weighed after closing, until they reached a constant weight for three consecutive weightings ( $\Delta w < \pm 0.0005$  g) (26). Equilibration time for each of the hydrated samples ranged from one ( $a_w = 0.12$ ) up to 30 days for the samples at the highest  $a_w$  ( $a_w = 0.99$ ). Note that for the latter group of samples it was necessary to brush the meat samples with a 0.02% solution of NaN<sub>3</sub> before hydration to avoid growth of molds and to carry out the whole rehydration under a laminar flow hood. The  $a_w$  of the equilibrated samples was checked by an Aqualab water activity meter (Decagon Devices Inc., Pullman, USA). Dry matter content was determined gravimetrically according to ref 27. Water content percentages are hereafter expressed on a dry matter basis.

Sorption isotherm data were analyzed using four different equations (eqs. 1–4) according, respectively, to the GAB (11), BET (10), Caurie (28), and Asbi and Baianu (29) models.

$$X = \frac{X_m C_G K a_w}{(1 - K a_w)[1 + (C_G - 1)K a_w]} \quad (1)$$

$$X = \frac{X_m C_b a_w}{(1 - a_w)[1 + (C_b - 1)a_w]} \quad (2)$$

$$\ln(X) = \ln(X_m C^{1/n}) + \frac{2C^{1/n}}{X_m} \ln \frac{a_w}{1 - a_w} \quad (3)$$

$$X = n_1 + C a_w + A a_w^B \quad (4)$$

In all equations,  $X$  is the sample water content percentage, and  $X_m$  is the percentage of water forming a monolayer of adsorbed water. In eq 1,  $C_G$  is the Guggenheim constant, and  $K$  is a constant related to the modified properties of the sorbate in the multilayer region; in eq 2,  $C_b$  is a constant related to the net heat of sorption; in eq 3,  $n$  is the number of adsorbed water layers, and  $C$  is a constant related to  $C_b$  in eq 2; finally, in eq 4, all parameters have a mere empirical meaning. The  $a_w$  value at which water condensation takes place was estimated (i) according to Caurie ( $a_{x_m}^2$ , 28) using eq 5

$$\frac{1}{a_{x_m}^2} = 1 + \frac{1}{X_m^{n/2}} \quad (5)$$

and (ii) from the intersection between the linear and power-law tract of eq 4 ( $n$  being close to zero, see **Table 1**).

**Table 1.** Parameters Obtained from the Fitting of Equations 1–4 to Chicken Breast Meat Sorption Isotherm Data

type of equation	best fit parameters	onset of moisture condensation
BET	$X_m = 6.31\%$ , $C_b = 1.715$	
GAB	$X_m = 6.04\%$ , $K = 0.9894$ , $C_G = 4.552$	
Caurie	$X_m = 4.00\%$ , $C^{1/n} = 1.78$ , $n = 2.25$	$a_w = 0.83$ (29.2%)
Ali Asbi and Baianu	$n_1 = 6.060 \times 10^{-3}$ , $C = 0.214$ , $A = 1.843$ , $B = 14.92$	$a_w = 0.86$ (39.7%)

**DSC Measurements.** Frozen water content was evaluated by a Pyris 6 DSC (Perkin-Elmer Corporation, Wellesley, USA). The DSC was equipped with a low-temperature cooling unit Intacooler II (Perkin-Elmer Corporation, Wellesley, USA). Temperature calibration was done with ion exchanged distilled water (mp 0.0 °C), indium (mp 156.60 °C), and zinc (mp 419.47 °C); heat flow was calibrated using the heat of fusion of indium ( $\Delta H = 28.71$  J/g). For the calibration, the same heating rate as used for sample measurements was applied under a dry nitrogen gas flux of 20 mL/min. Each sample (about 20 mg) was weighed in 50  $\mu$ l aluminum pans, hermetically sealed, and then loaded onto the DSC instrument at room temperature, using an empty pan of the same type for reference. Samples were then cooled at 5 °C/min to -60 °C, held for 1 h, and then scanned at 5 °C/min to 20 °C (30). Unfrozen water was evaluated, according to Quinn et al. (31), as the maximum water content for which no enthalpic peak is detected and obtained from the intercept at  $\Delta H = 0$  of a linear fit of the melting enthalpies vs water content percentages.

**NMR Relaxation Measurements.** Proton  $T_2$  of the samples was measured in triplicate at each moisture level. Samples of about 350 mg of meat were placed inside 10 mm o.d. NMR tubes in such a way that they did not exceed the active region of the RF coil, and they were analyzed at 24 °C with the CPMG pulse sequence using a Bruker Minispec PC/20 spectrometer operating at 20 MHz. Each measurement comprised 3000 points, corresponding to 3000 echoes, with a  $2\tau$  interpulse spacing (i.e., between each couple of 180° pulses) of 80  $\mu$ s and a recycle delay of 3.5 s. The number of scans was varied depending on moisture content, to obtain a S/N ratio in the range 900–1400. The CPMG decays corresponding to the same moisture content were normalized to the sample weight, averaged, and analyzed with the UPEN program (32). UPEN inverts the CPMG signal using a continuous model, that is, it finds the least biased distribution of transverse relaxation times that fits the CPMG decay at best according to eq 6

$$I(2\tau n) = \sum_{i=1}^M I_0(T_{2,i}) \exp(-2\tau n/T_{2,i}) \quad (6)$$

where  $2\tau$  is the CPMG interpulse spacing,  $n$  is the index of a CPMG echo, and  $I_0(T_{2,i})$  provides a distribution of signal intensities for each  $T_2$  component extrapolated at  $\tau = 0$  (the relaxogram), sampled logarithmically in the interval  $T_{2,\min} - T_{2,\max}$  set by the user. Default values for all UPEN parameters were used throughout this work. The behavior of UPEN in the presence of poorly sampled very fast relaxing signals together with slower components has been thoroughly studied by Moody and Xia (33); it was found that UPEN is able to reproduce good synthetic data of this type when  $S/N > 300$ , that is, well below the average S/N obtained in our experiments. Intensity of an NMR signal spanning a certain range of  $T_2$  values on the relaxogram was obtained from the fraction of the “cumulative signal percentage” provided by UPEN in that range, multiplied by the UPEN “total extrapolated NMR signal” (XSig).

It has been reported that when  $T_2 \ll T_{1\rho}$ , such as in tissues or gels, the CPMG sequence at short interpulse spacing may induce spin-lock and lead to a marked increase in the measured  $T_2$  values (15, 34). We have checked this possibility by comparing the relaxograms obtained by UPEN analysis of the CPMG and the alternating phase-CPMG (AP-CPMG, 35) decays of the same meat sample in the same conditions ( $2\tau = 80$   $\mu$ s) and found no significant differences. Because

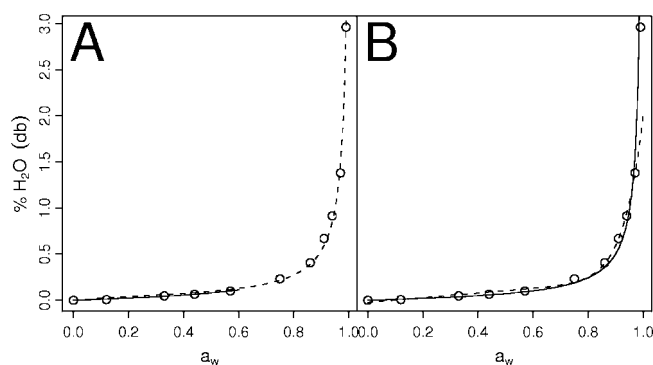


**Figure 1.** Moisture sorption isotherm of freeze-dried chicken breast meat at 25 °C. Experimental values (○); calculated values according to the GAB and BET models (dashed and solid, respectively, curves in panel A); calculated values according to the Asbi–Baianu and Caurie models (dashed and solid curves, respectively, in panel B).

the AP-CPMG sequence did not induce spin-lock in the sample (35), we conclude that all of our  $T_2$  measurements are not contaminated by  $T_{1\rho}$  effects. Similar results have been obtained (15) for cross-linked hydroxycellulose and carboxymethylcellulose networks.

**Deuteration Experiments.** The effect of deuteration on the  $T_2$  distribution of rehydrated chicken meat was studied using two freeze-dried samples weighting about 100 mg. The first sample was submitted to five consecutive hydration/freeze-drying cycles. In each cycle the sample was hydrated with a phosphate buffer solution in  $D_2O$  at pH 8 (to enhance H/D exchange), equilibrated in  $D_2O$  for about 15 min, and freeze-dried again. At the end of the fifth cycle the sample was weighed and rehydrated with the deuterated buffer solution so as to obtain a final moisture concentration typical of fresh meat ( $\approx 300\%$ ). The second sample (which we used as protonated reference) was treated in the same way as the first but used water instead of  $D_2O$ .

**Calibration of the NMR signal.** A calibration was attempted for determining the water content in meat from the measure of the absolute NMR CPMG signal intensity. Six samples of distilled  $H_2O$  spanning the range 52–398 mg were placed into 10 mm (o.d.) NMR tubes and were analyzed with the CPMG sequence, collecting 5000 echoes with an interpulse spacing of 2 ms and a recycle delay of 10 s. The 90° pulse was carefully checked for each of the calibration points and was found to be independent of the filling factor. This was expected, given the high homogeneity of the RF field within the several centimeters long solenoidal coil used in the Minispec probe (Fabio Tedoldi, Bruker Italy, private communication). Signal amplification was carefully adjusted along the series to take into account the different amounts of water in the samples and to prevent signal clipping. Because we had planned to use UPEN for the analysis of all of our meat signals, we calibrated the grams of water present into each sample versus the NMR signal using the total extrapolated NMR signal (XSig) parameter provided by UPEN after inversion of the water CPMG decays. A plot of the actual water content versus the intensity of the NMR signal yielded the straight line ( $R^2 = 0.9985$ ,  $P < 0.001$ ) described by eq 7,

$$\text{grams of } H_2O = (\text{XSig}' \times 5.4726 \times 10^{-4}) - 6.2876 \times 10^{-3} \quad (7)$$

where XSig' is the signal obtained by the UPEN XSig parameter and normalized to a Minispec amplification of 90. Equation 6 was found to correctly predict the weight of water in samples containing various amounts of 10 mM  $CuSO_4$  and 246 mM  $FeCl_3$  solutions (having  $T_2 = 162$  and 16 ms, respectively) with an average relative error of 3.7%. It was also assumed that the amount of the water population appearing in the leftmost part of the meat relaxograms (i.e., at shorter  $T_2$  values) could be predicted as reliably.

## RESULTS

**Sorption Isotherm.** The sorption isotherm for freeze-dried chicken breast meat at 25 °C is shown in **Figure 1** together

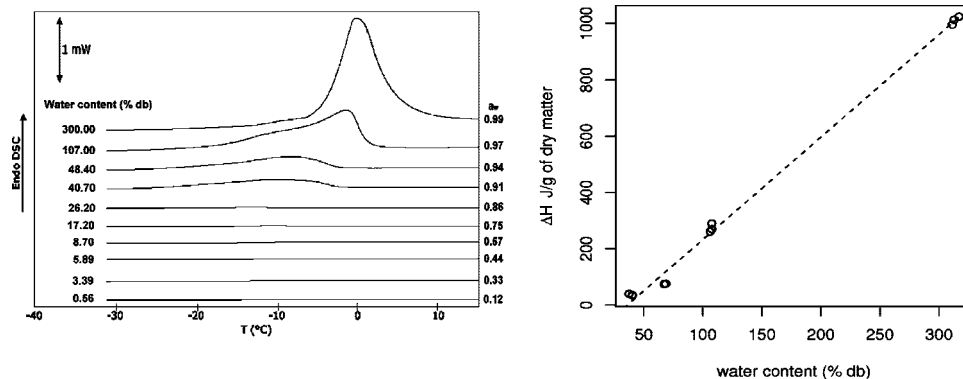


**Figure 2.** Sample heating scans of freeze-dried breast chicken meat hydrated at several water contents (left), and a linear fit of the corresponding melting enthalpies (in triplicate) vs. water content (right).

with the best-fit curves obtained through the BET or the GAB model (**Table 1**).

The monolayer values are, in both cases, smaller than found recently by Delgado and Sun (24) for the same foodstuff and temperature (7.34% and 6.75% for BET and GAB, respectively), probably because their data were obtained from a desorption isotherm.

Although the GAB equation is by far the most used mathematical model for the fitting of isotherm data, a plethora of other models exists, some of which yield physically meaningful parameters, whereas others are totally empirical and whose only aim is reconstructing the isotherm shape at best for engineering purposes. The recently modified Caurie equation (28) belongs to the first group of models. It is based on a modification of the BET equation, but, contrary to BET, the Caurie model does not allow an infinite number of water layers to be adsorbed over the first. Consequently, an end-point for adsorption of water molecules can be marked, which corresponds to the  $a_w$  point at which bulk water appears. On the opposite side, one of the simplest empirical models able to describe the shape of an isotherm is that of Asbi and Baianu (29). They noted that most food isotherms are of type II in the Brunauer classification (3) and fitted the experimental points with a simple equation (eq 4, in the Materials and Methods section). The Asbi and Baianu model is useful in that it provides a simple way for marking the beginning of the isotherm upswing from the intersection between the linear and the power-law part of eq 4.

The best-fit parameters for the Caurie and Asbi and Baianu models are reported in **Table 1**, together with the estimated water activities at which moisture condensation takes place. It appears that above  $a_w = 0.83$ – $0.86$  meat water should be considered as bulk-like; given the difference between the two models, the agreement is remarkable. Note that our Caurie monolayer value is lower than both BET and GAB estimates, as also recently found for goat meat (36) and spent hen meat (37). Therefore, the Caurie (38) notion that monolayer values obtained from eq 3 are usually larger than BET values must not be taken for granted, at least for meat samples.

**DSC.** Heating scans of the same chicken meat samples used for the sorption isotherm are shown in **Figure 2**. It is apparent that up to  $a_w = 0.86$  (26.2% water content) no endothermic peak is detected, meaning that only “unfrozen water” (usually believed to be water bound to the macromolecular matrix with a mobility so limited that it cannot freeze) exists in those samples. Only above  $a_w = 0.86$  is an endothermic peak detected at about  $T = -15$  °C, which gradually increases and moves toward  $T = 0$  °C with sample hydration.

According to Quinn et al. (31), total bound water corresponds to the maximum water content for which no enthalpic peak is detected and can be obtained from the intercept at  $\Delta H = 0$  of a linear fit of the melting enthalpies versus water content percentages (**Figure 2**). From the fitting equation,  $\Delta H = 3.639 \times W - 130.8$  (where  $\Delta H$  is the melting enthalpy per gram of dry matter, and  $W$  is the moisture percentage), the unfrozen water content of 35.9% is estimated; note that the slope of the fitting equation ( $363.9 \text{ J g}^{-1}$ ) does not equal the melting enthalpy of pure water ( $334 \text{ J g}^{-1}$ ), thus confirming the notion (31) that the amount of frozen water cannot be calculated from the melting peak area using the heat of fusion of pure water.

**NMR.** The results of UPEN inversion (32) of the CPMG data obtained from freeze-dried chicken meat samples equilibrated at several  $a_w$  values are shown in **Figure 3A**. At every water content the  $T_2$  relaxograms comprise a major water population whose average  $T_2$  starts from about 0.2 ms at low hydration and gradually moves toward the “standard” value of 30–50 ms for raw meat (39, 40).

The width of the main peak also changes with water content, although not as monotonically. In fact, at  $a_w = 0.75$  (corresponding to a water content of 17.2%), a sudden narrowing of the main water peak takes place, together with a shift to higher  $T_2$  values, which is diagnostic of enhanced water mobility; a shoulder at about  $T_2 = 0.3$  ms is also uncovered, revealing a faster-relaxing proton population (**Figure 3B**). At  $a_w = 0.86$  (water content 26.2%), the new peak is completely visible. At  $a_w = 0.99$  (water content 300%) the relaxogram resembles that of fresh meat.

A discontinuity is also observed in the plot of the major peak relaxation rate ( $R_2 = T_2^{-1}$ ) versus moisture percentage (**Figure 4**); an estimate (41) of the slope break-point through linear fitting of 4 experimental points at low hydration and 3 points at high hydration yields 17.8%, a moisture content close to that at which the shoulder appears.

## DISCUSSION

According to Wolfe et al. (18), hydration water of macromolecules or biomembranes is the one “whose physical properties [...] become different from those of pure water”. Under this view, both our DSC and isotherm data point toward a situation where up to 30–40% of moisture water can be considered as “different from pure water” either because of low  $a_w$  or its inability to freeze at 0 °C. The value of 35.9% of unfrozen water provided by DSC lays within the range of estimated moisture contents at which bulk water appears (**Table 1**), thus confirming that both techniques detect the same hydration process. On the other side, the NMR results shown

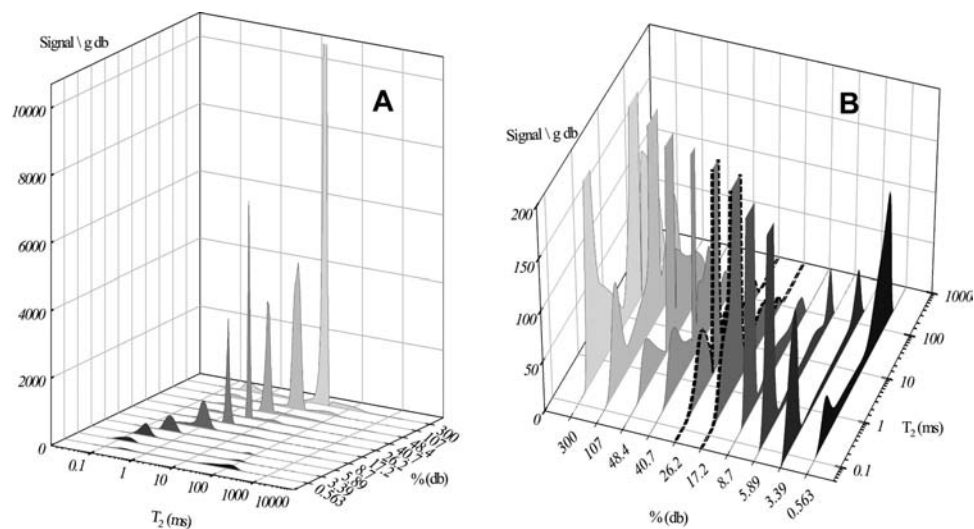


**Figure 3.** (A)  $T_2$  relaxograms of freeze-dried chicken breast meat samples rehydrated at several water contents. (B) Close-up view showing the appearance of the fast-relaxing shoulder at  $a_w = 0.75$  (17.2%).

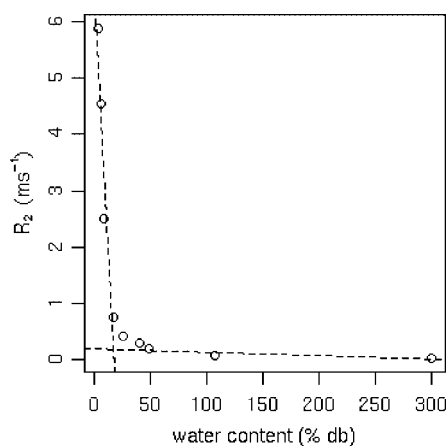


**Figure 4.** Relaxation rate vs water percentage in freeze-dried chicken meat sample at several moisture contents. The two dashed lines cross at 17.8%.

in **Figure 4** seem to contradict the above agreement because mobile water appears where it is reported by DSC to be still unfrozen (i.e., in the range 17.2–35.9%). Similar phenomena have been noted in starch and cellulose systems and are ascribed to the presence of “metastable water” (12). However, a simpler explanation is possible here. Water in meat may not freeze before 35.9% simply because the contemporary presence of small solutes, membranes, and macromolecules depresses the freezing point according to mechanisms (i) and (ii) described in the Introduction section; thus, no DSC peak is visible between 17.2 and 35.9% of moisture despite water not actually being bound.

By looking at the plot in **Figure 4** it is clear that water mobility is very limited at low hydration. The high relaxation rate is the result of a combined effect of the higher water correlation time, due to the slower reorientation of water close to the mesoscopic meat structures (18), and cross exchange of hydration water with the extremely fast relaxing exchangeable matrix protons. Therefore, in the first part of **Figure 4**, before the break point,  $R_2$  decreases probably because the plasticizing effect of the added water enhances matrix mobility, thus reducing the  $R_2$  of the matrix protons (exchangeable matrix protons included), in turn also reducing the main water population  $R_2$  via proton exchange. After hydration completes, although the matrix has reached its maximum mobility,  $R_2$  keeps

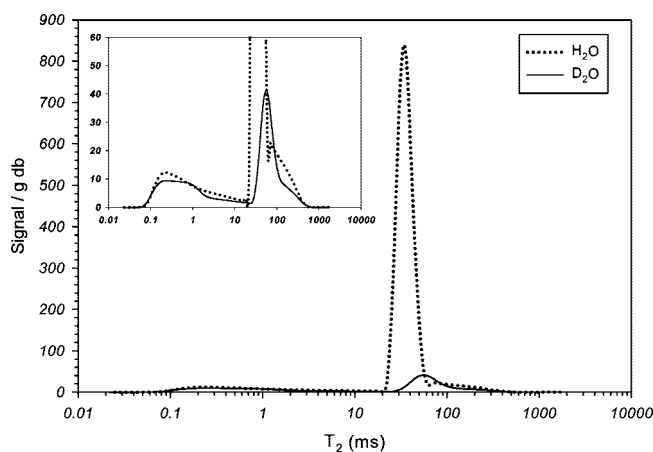


**Figure 5.**  $T_2$  relaxograms of two samples of the same freeze-dried chicken breast meat rehydrated to  $a_w = 0.99$  in  $H_2O$  (dotted line) and  $D_2O$  (solid line). A close-up view of the fast-relaxing part is shown in the inset.

decreasing (albeit with a lower dependence on moisture content) because of exchange between the increasing amount of bulk water and water entrapped in matrix cavities (42) and/or labile matrix protons (43).

The small population of fast-relaxing protons peaking at about  $T_2 = 0.2$  ms and appearing at 17.2% moisture is usually assigned to water tightly associated with the matrix macromolecules, although it has been noted that some part of this signal may also come from protons of the macromolecular matrix (44, 45). We have reinvestigated this old result and rehydrated lyophilized meat in  $D_2O$  and  $H_2O$  (see the Materials and Methods section). Analysis of the corresponding relaxograms (**Figure 5**) shows that as much as 83.4% of the total signal at low  $T_2$  persists in  $D_2O$ .

A similar experiment has been recently reported (46) where no difference in the population of the fast-relaxing signal fraction was detected upon deuteration; it was concluded that this fraction originated from protons not susceptible to exchange, that is, hydration water (46). We note however that this fraction is also minimally affected by meat homogenization, which disrupts the overall meat structure (44) and should indeed significantly modify the amount of the hydration water held by the matrix. Thus, we believe that another explanation for the origin of the fast-relaxing fraction in meat relaxograms is possible. In fact, in a recent work about heat-set BSA gels prepared in  $H_2O$  and

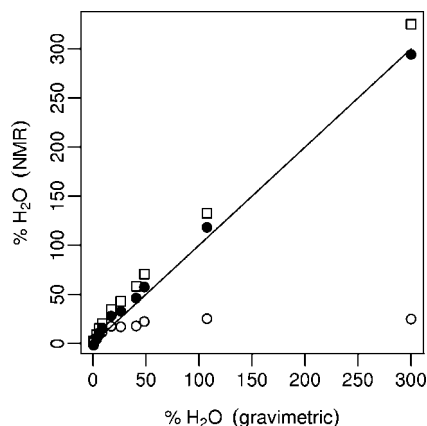


**Figure 6.** Comparison between actual water content and water content inferred from NMR signal through a reference calibration: (■) values obtained from total NMR signal; (●) values obtained from the NMR signal after subtracting the fast-relaxing signal population; (○) difference between water obtained from total NMR signal and actual value.

D<sub>2</sub>O (whose relaxograms resemble that of fresh meat, 44), some of us assigned the low-T<sub>2</sub> signal to macromolecular protons located in water-plasticized structures (47). Further, the decrease of the low-T<sub>2</sub> signal in D<sub>2</sub>O matched the percentage of exchangeable protons in BSA. The fact that separate populations for water and exchangeable protein protons were detected in BSA gels is not surprising, because a proton exchange constant of the order of 2000 s<sup>-1</sup> has been reported for cross-linked BSA (48), which is quite slow with respect to either the fast-relaxing protons average relaxation rate (about 1 × 10<sup>4</sup> s<sup>-1</sup>) or to the reciprocal 2τ space we used for the CPMG experiments (1.25 × 10<sup>4</sup> s<sup>-1</sup>). Because BSA gels have been proposed as models for the study of the NMR relaxation properties of tissues (49), it seems reasonable to extend our previous BSA findings (47) to meat and to assign the low T<sub>2</sub> signal in meat to protons located on macromolecular structures plasticized by water. The fraction disappearing in D<sub>2</sub>O is assigned, again by comparison with BSA experiments (47), to exchangeable protons located on the plasticized structures.

A further proof that the low-T<sub>2</sub> signal is due to protons exceeding those added with water is obtained from a comparison between the gravimetric water content and the water content inferred from the total NMR signal through a reference calibration (see Materials and Methods section). It appears that the water content obtained from the total NMR signal is higher than the actual (Figure 6).

Subtraction of the low-T<sub>2</sub> signal population from total NMR signal, where possible (i.e., for samples at hydration higher or equal to 17.2%), greatly improves the agreement. It is also instructive to note that the difference between NMR- and gravimetrically measured protons is not constant but gradually increases with moisture until it reaches a plateau at 17.2% of actual hydration (Figure 6). Beyond this point, the difference between NMR-inferred and actual water content is, on the average, 20.8%, that is, about 6.4% of the total meat NMR CPMG signal. This behavior is again compatible with a model by which the solid matrix (whose NMR signal decays too fast to be detected by CPMG experiments in our conditions) is gradually plasticized by water and becomes more and more detectable in the low-T<sub>2</sub> region of the relaxograms as hydration proceeds. As soon as hydration is complete, plasticized chains have reached their maximum amount and mobility and do not change further upon water addition. Our explanation is corroborated by the results very recently published for model

systems of cross-linked proteins (50) for which a positive deviation between water, inferred by NMR and by gravimetry, was always obtained at high hydration, that is, where side chain mobility was high as confirmed by dramatic reduction of the proteins second moment.

In conclusion, the study of water dynamic during the hydration of freeze-dried chicken breast meat through a multianalytical approach revealed an agreement (between sorption isotherm and DSC experiments) and an apparent contradiction (between NMR and the other experiments) concerning the water content at which mobile water appears (30–40% for DSC and isotherm, and 17.2% for NMR). This contradiction can be reconciled by noting that frozen water may not appear in DSC experiments because the presence of solutes and mesoscopic objects may depress the water freezing point so that it cannot form ice in our DSC conditions, for thermodynamic reasons. We have also put forward the proposal that the fastest-relaxing part of the NMR signal detected in T<sub>2</sub> relaxograms of chicken breast meat may not arise from the usually invoked structural water, but from matrix protons located in meat structures that are plasticized by the addition of water; this view is strengthened by our finding that on the average 6.4% of the total <sup>1</sup>H CPMG-NMR signal of chicken breast meat is not due to the added water. Further studies are in progress in our laboratory for relating our findings on water dynamics in chicken meat to the extent of physicochemical and biological reactions bound to meat safety and stability.

#### LITERATURE CITED

- (1) Vittadini, E.; Dickinson, L. C.; Lavoie, J. P.; Pham, X.; Chinachoti, P. Water mobility in Multicomponent Model Media As Studied by <sup>2</sup>H and <sup>17</sup>O NMR. *J. Agric. Food Chem.* **2003**, *51*, 1647–1652.
- (2) Van den Berg, C.; Bruin, S. Water activity and its estimation in food systems. Theoretical aspects. In *Water activity: Influences on food quality*; Rockland, L. B., Stewart, G. F., Eds.; Academic Press: New York, 1981; 1–43.
- (3) Al-Muhtaseb, A. H.; McMinn, W. A. M.; Magee, T. R. A. Moisture sorption isotherm characteristics of food products: a review. *Food Bioprod. Process.* **2002**, *80*, 118–128.
- (4) Labuza, T. P.; McNally, L.; Gallangher, D.; Hawkes, J.; Hurtado, F. Stability of intermediate moisture foods: 1. Lipid oxidation. *J. Food Sci.* **1972**, *37*, 154–159.
- (5) Mateus, M.-L.; Rouvet, M.; Gumy, J.-C.; Liardon, R. Interactions of Water with Roasted and Ground Coffee in the Wetting Process Investigated by a Combination of Physical Determinations. *J. Agric. Food Chem.* **2007**, *55*, 2979–2984.
- (6) Hossain, M. A.; Ishihara, T.; Hara, K.; Osatomi, K.; Ali Khan, M. A.; Nozaki, Y. Effect of Proteolytic Squid Protein Hydrolysate on the State of Water and Dehydration-Induced Denaturation of Lizard Fish Myofibrillar Protein. *J. Agric. Food Chem.* **2003**, *51*, 4769–4774.
- (7) Bertram, H. C.; Whittaker, A. K.; Andersen, H. J.; Karlsson, A. H. pH Dependence of the Progression in NMR T<sub>2</sub> Relaxation Times in Post-mortem Muscle. *J. Agric. Food Chem.* **2003**, *51*, 4072–4078.
- (8) Morillon, V.; Debeaufort, F.; Capelle, M.; Blond, G.; Voilley, A. Influence of the Physical State of Water on the Barrier Properties of Hydrophilic and Hydrophobic Films. *J. Agric. Food Chem.* **2000**, *48*, 11–16.
- (9) Slade, L.; Levine, H. Beyond water activity: recent advances based on an alternative approach to the assessment of food quality and safety. *CRC Critical Rev. Food Sci. Nutri.* **1991**, *30*, 115–360.
- (10) Brunauer, S.; Emmet, P. H.; Teller, E. Adsorption of gases in multimolecular layers. *J. Am. Chem. Soc.* **1938**, *60*, 309–319.
- (11) Anderson, R. B. Modification of the B. E. T. equation. *J. Am. Chem. Soc.* **1946**, *68*, 686–691.

- (12) Li, S.; Dickinson, L. C.; Chinachoti, P. Mobility of “unfreezable” and “freezable” water in waxy corn starch by  $^2\text{H}$  and  $^1\text{H}$  NMR. *J. Agric. Food Chem.* **1998**, *46*, 62–71.
- (13) Cornillon, P. Characterization of osmotic dehydrated apple by NMR and DSC. *Lebensm.-Wiss. Technol.* **2000**, *33*, 261–267.
- (14) Ping, Z. H.; Nguyen, Q. T.; Chen, S. M.; Zhou, J. Q.; Ding, Y. D. States of water in different hydrophilic polymers – DSC and FTIR studies. *Polymer* **2001**, *42*, 8461–8467.
- (15) Capitani, D.; Mensitieri, G.; Porro, F.; Proietti, N.; Segre, A. L. NMR and calorimetric investigation of water in a superabsorbing crosslinked network based on cellulose derivatives. *Polymer* **2003**, *44*, 6589–6598.
- (16) Pitombo, R. N. M.; Lima, G. A. M. R. Nuclear magnetic resonance and water activity in measuring the water mobility in Pintado (*Pseudoplatystoma corruscans*) fish. *J. Food Eng.* **2003**, *58*, 59–66.
- (17) Simatos, D.; Faure, M.; Bonjour, E.; Couach, M. Differential thermal analysis and differential scanning calorimetry in the study of water foods. In *Water Relations of Foods*; Duckworth, R. D., Ed.; Academic Press: London, United Kingdom, 1975, 193.
- (18) Wolfe, J.; Bryant, G.; Koster, K. L. What is ‘unfreezable water’, how unfreezable is it and how much is there? *CryoLetters* **2002**, *23*, 157–166.
- (19) Kantor, Z.; Pitsi, G.; Thoen, J. Glass transition temperature of honey as a function of water content as determined by differential scanning calorimetry. *J. Agric. Food Chem.* **1999**, *47*, 2327–2330.
- (20) Tocci, A. M.; Mascheroni, R. H. Characteristic of differential scanning calorimetry determination of thermophysical properties of meats. *Lebensm. Wissen. Technol.* **1998**, *31*, 418–426.
- (21) Hills, B. P. Applications of low-field NMR to food science. *Annu. Rep. NMR Spectrosc.* **2006**, *58*, 177–230.
- (22) Bertram, H. C.; Andersen, H. J. Application of NMR in meat science. *Annu. Rep. NMR Spectrosc.* **2004**, *53*, 157–202.
- (23) Aktaş, N.; Tülek, Y.; Gökalp, H. Y. Determination of differences in free and bound water contents of beef muscle by DSC under various freezing conditions. *J. Therm. Anal. Calorim.* **1997**, *50*, 617–624.
- (24) Delgado, A. E.; Sun, D.-W. Desorption isotherms and glass transition temperature for chicken meat. *J. Food. Eng.* **2002**, *55*, 1–8.
- (25) Bell, L. N.; Labuza, T. P. In *Practical Aspects of Moisture Sorption Isotherm Measurement and Use, 2nd Ed.*; AACC Egan Press, Egan, Minnesota, 2000.
- (26) Spiess, W. E. L.; Wolf, W. R. The results of the COST 90 Project on water activity. In *Physical Properties of Foods*, Jowitt, R., Escher, F., Hallström, B., Meffert, H. F., Spiess, W. E. L., Vos G. Eds.; London and New York, Applied Science Publishers: London, 1983, 65–91.
- (27) Anonymous, method no. 950.46. In *Official Methods of Analysis, edition 15*; Association of Official Analytical Chemists: Arlington, Virginia, 1990.
- (28) Caurie, M. The unimolecular character of the classical Brunauer, Emmett and Teller adsorption equation and moisture adsorption. *Int. J. Food Sci. Technol.* **2005**, *40*, 283–293.
- (29) Asbi, B. A.; Baianu, I. C. An equation for fitting moisture sorption isotherms of food proteins. *J. Agric. Food Chem.* **1986**, *34*, 494–496.
- (30) Brake, N. C.; Fennema, O. R. Glass Transition Values of Muscle Tissue. *J. Food Sci.* **1999**, *64*, 10–15.
- (31) Quinn, F. X.; Kampff, E.; Smyth, G. McBrierty, V. J. Water in hydrogels. 1. A study of water in poly(N-vinyl-2-pyrrolidone/methyl methacrylate) copolymer. *Macromolecules* **1988**, *21*, 3191–3198.
- (32) Borgia, G. C.; Brown, R. J. S.; Fantazzini, P. Uniform-Penalty Inversion of Multiexponential Decay Data. *J. Magn. Reson.* **1998**, *132*, 65–77.
- (33) Moody, J. B.; Xia, Y. Analysis of multi-exponential relaxation data with very short components using linear regularization. *J. Magn. Reson.* **2004**, *167*, 36–41.
- (34) Santyr, G. E.; Henkelman, M. J.; Bronskill, R. M. Variation in measured transverse relaxation in tissue resulting from spin locking with the CPMG sequence. *J. Magn. Reson.* **1988**, *79*, 28–44.
- (35) Suh, B. J.; Torgeson, D. R.; Borsa, F. Fluxon thermal motion detected by nuclear spin echo decay measurements:  $^{89}\text{Y}$  NMR in  $\text{YBa}_2\text{Cu}_3\text{O}_7$ . *Phys. Rev. Lett.* **1993**, *71*, 3011–2014.
- (36) Singh, R. R. B.; Rao, K. H.; Anjaneyulu, A. S. R.; Patil, G. R. Water desorption characteristics of raw goat meat: effect of temperature. *J. Food Eng.* **2006**, *75*, 228–236.
- (37) Singh, R. R. B.; Rao, K. H.; Anjaneyulu, A. S. R.; Patil, G. R. Moisture properties of smoked chicken sausages from spent hen meat. *Food Res. Int.* **2001**, *34*, 143–148.
- (38) Caurie, M. Derivation of full range moisture sorption isotherms. In *Water Activity: Influences on Food Quality*; Rockland, L. B., Stewart, G. F., Eds.; Academic Press: NY, 1981; 63–87.
- (39) Brown, R. J. S.; Capozzi, F.; Cavani, C.; Cremonini, M. A.; Petracci, M.; Placucci, G. Relationships between  $^1\text{H}$  NMR relaxation data and some technological parameters of meat: a chemometric approach. *J. Magn. Reson.* **2000**, *147*, 89–94.
- (40) Bertram, H. C.; Dønstrup, S.; Karlsson, A. H.; Andersen, H. J. Continuous distribution analysis of  $T_2$  relaxation in meat — an approach in the determination of water-holding capacity. *Meat. Sci.* **2002**, *60*, 279–285.
- (41) Vackier, M.-C.; Hills, B. P.; Rutledge, D. N. An NMR relaxation study of the state of water in gelatin gels. *J. Magn. Reson.* **1999**, *138*, 36–42.
- (42) Vaca Chávez, F.; Persson, E.; Halle, B. Internal water molecules and magnetic relaxation in agarose gels. *J. Am. Chem. Soc.* **2006**, *128*, 4902–4910.
- (43) Vaca Chávez, F.; Hellstrand, E.; Halle, B. Hydrogen exchange and hydration dynamics in gelatin gels. *J. Phys. Chem. B* **2006**, *110*, 21551–21559.
- (44) Bertram, H. C.; Karlsson, A. H.; Rasmussen, M.; Pedersen, O. D.; Dønstrup, S.; Andersen, H. J. Origin of multiexponential  $T_2$  relaxation in muscle myowater. *J. Agric. Food Chem.* **2001**, *49*, 3092–3100.
- (45) Peemoeller, H.; Pintar, M. M. Nuclear magnetic resonance multiwindow analysis of proton local fields and magnetization distribution in natural and deuterated mouse muscle. *Biophys. J.* **1979**, *28*, 339–355.
- (46) Bertram, H. C.; Andersen, H. J. Proton NMR relaxometry in meat science. In *Modern Magnetic Resonance*; Webb, G. A. Ed.; Springer: Dordrecht, Netherlands, 2006, 1707–1711.
- (47) Cremonini, M. A.; Venturi, L.; Sýkora, S.; Cavani, C.; Placucci, G. Reference convolution of low resolution FIDs in the presence of poor magnetic field homogeneity. *Magn. Res. Imag.* **2007**, *25*, 555.
- (48) Hills, B. P.; Takacs, S. F.; Belton, P. S. The effect of proteins on the proton N.M.R. transverse relaxation time of water. II. Protein aggregation. *Mol. Phys.* **1989**, *67*, 919–937.
- (49) Koenig, S. H.; Brown, R. D., 3rd. A molecular theory of relaxation and magnetization transfer: application to cross-linked BSA, a model for tissue. *Magn. Res. Med.* **1993**, *30*, 685–695.
- (50) Diakova, G.; Goddard, Y. A.; Korb, J.-P.; Bryant, R. G. Changes in protein structure and dynamics as a function of hydration from  $^1\text{H}$  second moment. *J. Magn. Reson.* **2007**; doi 10.1016/j.jmr.2007.09.005.

---

Received for review September 27, 2007. Accepted October 18, 2007.

JF072874B